Photoswitchable Covalent Adaptive Networks Based on Thiol−Ene Elastomers

Kezi Cheng, Alex Chortos,* Jennifer A. Lewis, and David R. Clarke*

Cite This: https://doi.org/10.1021/acsami.1c22287

Read Online

ACCESS | Metrics & More | Article Recommendations | Supporting Information

ABSTRACT: Covalent adaptive networks combine the advantages of cross-linked elastomers and dynamic bonding in a single system. In this work, we demonstrate a simple one-pot method to prepare thiol−ene elastomers that exhibit reversible photoinduced switching from an elastomeric gel to fluid state. This behavior can be generalized to thiol−ene cross-linked elastomers composed of different backbone chemistries (e.g., polydimethylsiloxane, polyethylene glycol, and polyurethane) and vinyl groups (e.g., allyl, vinyl ether, and acrylate). Photoswitching from the gel to fluid state occurs in seconds upon exposure to UV light and can be repeated over at least 180 cycles. These thiol−ene elastomers also exhibit the ability to heal, remold, and serve as reversible adhesives.

KEYWORDS: covalent adaptive network, elastomer chemistry, click chemistry, self-healing, photoresponsive materials, adhesives
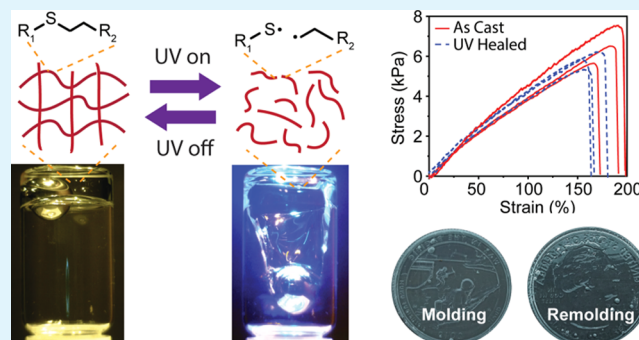
1. INTRODUCTION

Elastomeric materials are widely used in soft robotics,[1−4] conformable electronics,[5,6] adhesives,[7−9] and rubbers.[10] Typically, once set, their covalently cross-linked networks cannot be reprocessed. Yet, this capability enables remolding,[11,12] error correction,[13] self-healing,[14−18] and recycling.[19−21] Although cross-linked networks can undergo bond cleavage or depolymerization at high temperatures or under specific chemical conditions, this typically leads to a concomitant degradation of their mechanical properties.[22] By contrast, covalent adaptable networks[23] (CANs), which rely on reversible, click-like chemistry, exhibit mechanical robustness and creep resistance of photosets coupled with the plasticity and reprocessing ability of thermoplastics when triggered by external stimuli, such as thermal,[24−30] chemical stimuli,[31,32] and light.[33−36]

Light-based CANs have the advantage that the stimulus can be applied and removed quickly under ambient conditions.[37] Two approaches have been demonstrated: (1) dimerization reactions that result in changes to the network bond density that persist in the absence of stimuli[35,38] and (2) radical-mediated bond reshuffling in which the bonds become dynamic during optical stimulation but become static in the absence of stimulation.[33,34,39,40] The latter strategy results in fast reorganization of the network because a single generated radical can lead to the reorganization of multiple bonds while still preserving the total number of bonds. Recently, radical-induced light-based CANs have enabled new functionalities in tough composites[41] and adaptive soft actuators.[42,43] However, these systems require the implementation of specific chemical moieties (e.g., allyl sulfide or trithiocarbonate) into the polymer compositions. Achieving photoswitching in chemically simple systems, as shown here, would broaden their use in a myriad of applications.

Beyond inducing dynamic properties, light is widely used to cross-link polymer networks. As one of the most prevalent photocuring chemistries, thiol−ene coupling[44,45] leverages the high-yield reaction between thiol groups (R$_1$−S−H) and alkene groups (C=C−R$_2$) to form alkyl sulfides (R$_1$−S−C−C−R$_2$). This step growth process proceeds via the propagation of a thiyl radical through a vinyl functional group and regenerates the thiyl radical from a free thiol.[44,45] Due to their rapid reaction rates and relatively low sensitivity to oxygen,[46] thiol−enes have been used to cross-link polymer backbones that contain other types of dynamic bonds.[12,35,47] In addition, thiol−ene coupling can be chemically catalyzed via thiol-Michael reactions. Such reactions have recently been shown to be thermally reversible, enabling thermal CANs to be synthesized from simple precursors.[48,49]

Here, we report that light-induced, radical-mediated dynamic bonding can occur in thiol−ene elastomer networks, referred to as photo-CANs, which can be readily synthesized from low-cost, simple precursors. The desired behavior arises due to the dynamic nature of sulfide bonds in the presence of radicals.[50−54] In the absence of UV light, these elastomers exhibit typical
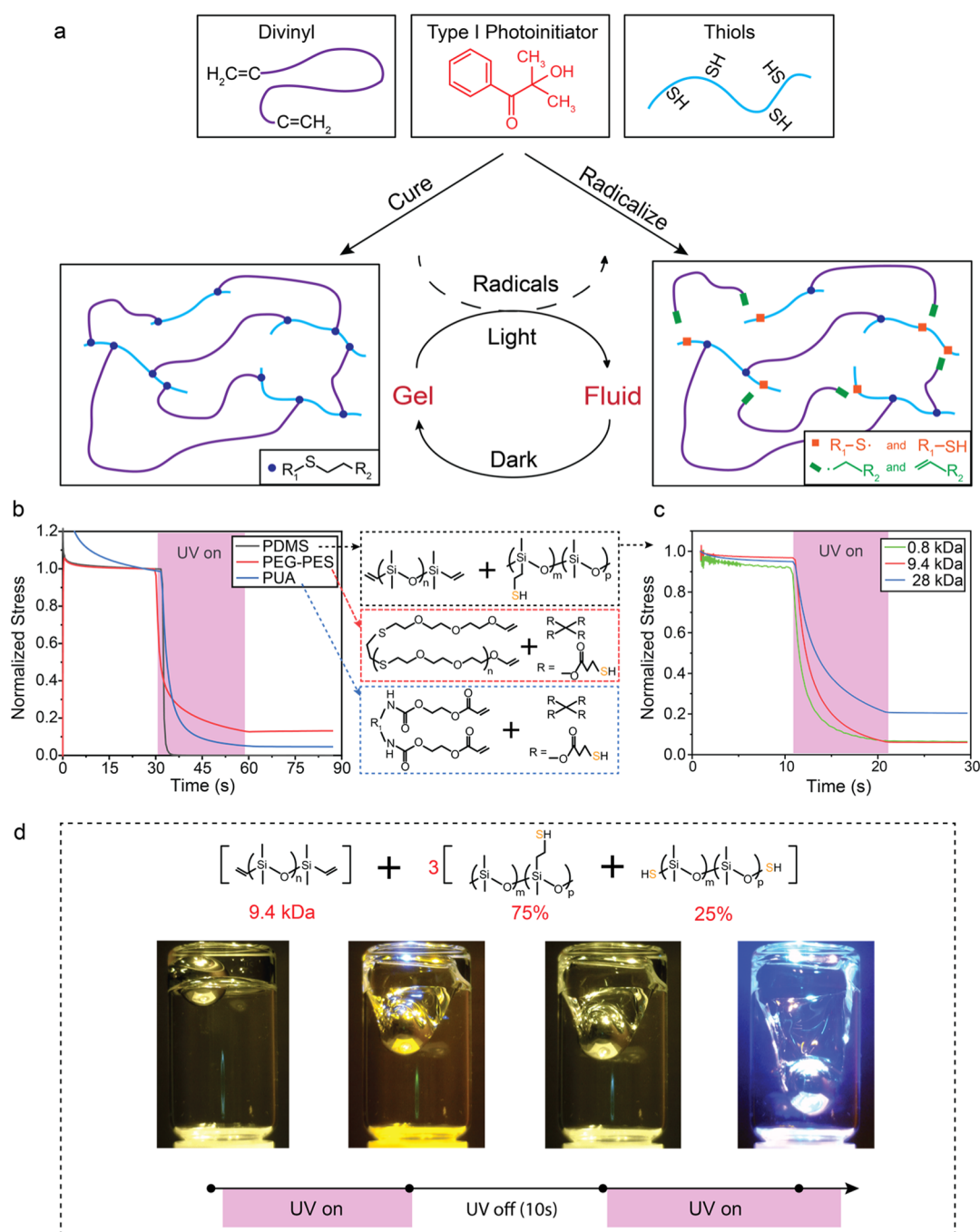
Figure 1. (a) Schematic illustration of radical-mediated photoswitching of thiol−ene elastomers from a gel network to a fluid (sol) state. (b) Stress relaxation measurements showing the generality of the UV-induced switching in thiol−ene networks using different polymer backbones and vinyl chemistries at an intensity of 16.7 mW/cm². (c) Stress relaxation measurements with divinyl siloxanes of varying molecular weights. (d) PDMS-based photo-CAN resides in the fluid state when illuminated, allowing the metal sphere to fall under gravity. However, when the UV light is turned off, the photo-CAN resolidifies into a high viscosity gel that holds the sphere in place.

properties of covalently cross-linked elastomers, including low hysteresis, low creep, and excellent temperature stability. However, upon UV excitation, they exhibit rapid stress relaxation, flow, and healing. Their repeated transition from the gel-to-sol state is observed for more than 180 cycles of off/on switching of UV light.

2. RESULTS AND DISCUSSION

Photo-CANs are prepared using bifunctional vinyl oligomers and multifunctional thiol oligomers with Norrish type I

photoinitiators (Figure 1a). The composition begins as a solution (sol). When exposed to UV, radicals generated from the initiators catalyze the reaction of thiol and ene groups to form sulfide bonds and the composition forms a solid elastomer when the UV is turned off. When the UV is turned on again, the elastomer changes back to the sol state, where it behaves like a viscous liquid. We demonstrate the generality of UV-induced dynamic bonding in thiol−ene networks using stress relaxation measurements on elastomer compositions with a wide diversity of backbone chemistries and vinyl groups (Figure 1b). Backbone
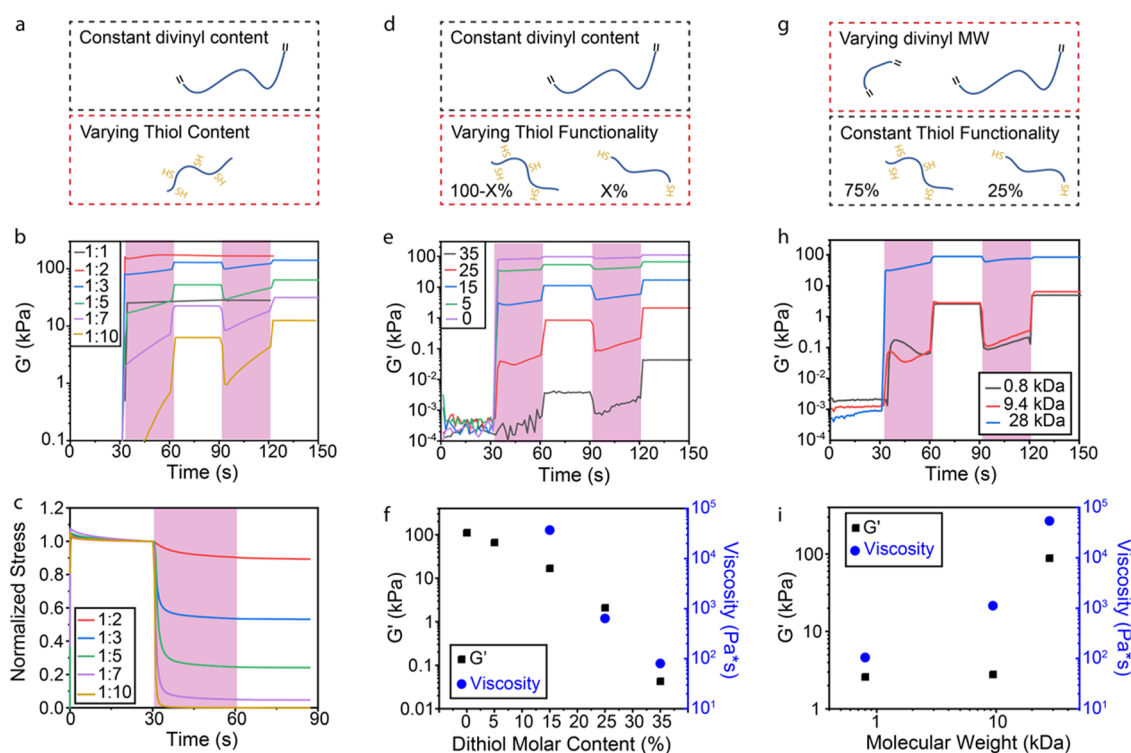
Figure 2. (a) Schematic of photo-CANs with a constant divinyl content and a varying thiol content with a 4.75 functional thiol oligomer. (b) G' vs time during photoswitching for systems with different vinyl/thiol ratios. (c) Stress relaxation during photoswitching for systems with different vinyl/thiol ratios. (d) Schematic of photo-CANs with a constant vinyl/thiol ratio of 1:3 and a varying thiol functionality. (e) G' vs time during photoswitching for systems with different dithiol contents. The legend indicates the molar content of dithiols in %. (f) G' (UV off) and viscosity (UV on) as a function of dithiol molar content. (g) Schematic of photo-CANs with a constant polythiol/dithiol ratio of 75:25 and a varying molecular weight of the divinyl oligomer. [Note: the sample denoted 0.8 kDa is prepared with a vinyl/thiol ratio of 1:2, while the 9.4 and 28 kDa samples are prepared with a vinyl/thiol ratio of 1:3.] (h) G' vs time during photoswitching for systems with different divinyl molecular weights. (i) G' (UV off) and viscosity (UV on) for systems with different divinyl molecular weights. In (b,c,e,h), the transparent magenta regions indicate that UV is turned on.

chemistries consisted of polydimethylsiloxane (PDMS), poly-(ethylene glycol-ethylene sulfide) (PEG-PES[55]), and polyurethane diacrylates (PUAs) with vinyl groups of allyl, vinyl ether, and acrylate, respectively. In all the compositions, nearly complete stress relaxation occurs within 30 s of UV exposure. Additionally, during 10 s of low-intensity UV exposure (3.65 mW/cm²), 0.8 and 9.4 kDa PDMS divinyl samples exhibited ~90% stress relaxation, while the 28 kDa sample relaxed by ~80% (Figure 1c). This short UV exposure corresponds to a dose of only 36.5 mJ/cm². Figure 1d vividly illustrates the effect of UV illumination on the viscosity of an optimized photo-CAN elastomer with a 9.4 kDa divinyl PDMS backbone, 1:3 vinyl/thiol ratio, and 75:25 ratio of polythiol/dithiol groups. In a variant of the classic Stokes experiment, a steel ball (8.2 g) is encased in the cured elastomer inside a glass vial. When the UV is off and the glass vial is turned upside down, the elastomer supports the steel ball against gravity. However, upon UV illumination for 10 s, the steel ball moves downward due to a sharp decrease in elastomer viscosity. When the UV light source is turned off for 10 s, the steel ball remains solidified in place indicating that the elastomer has returned to its original solid (gel) state (Video S1).

We explored the effects of the photo-CAN composition using photorheology measurements. We focused on PDMS-based systems due to the availability of oligomers with a wide range of molecular weights and functionalities. To probe compositional effects on photoswitching, we systematically varied the ratio of vinyl-to-thiol moieties, thiol functionality, and divinyl molecular

weight. The effect of the vinyl/thiol ratio was investigated using a divinyl oligomer with a molecular weight of 9.4 kDa (Figure 2a). The vinyl/thiol ratio is varied from 1:1 to 1:10 by adding different amounts of a thiol-functionalized oligomer with a functionality of ~4.75 (polythiol). Elastomers with a thiol ratio of 1:1 and 1:2 (near ideal stoichiometry) exhibited no photoswitching behavior, as reflected by a near constant value of the storage modulus (G') (Figures 2b and S1). For thiol contents greater than 1:3, G' quickly decreases upon UV exposure due to the radical-induced dynamic properties of the sulfide bonds. The slow increase of G' during UV exposure is hypothesized to be caused by the photoinduced depletion of initiators (reduction in the concentration of radicals) and the occurrence of side reactions that induce the formation of carbon−carbon cross-links that are not dynamic (Figure S2).[56,57] In this range of thiol contents greater than 1:3, the photoinduced change in the storage modulus increased with the thiol content, while the G' in the solid state (UV off) decreased. Stress relaxation measurements corroborate the increased plasticity of the matrix with an increasing degree of stress relaxation at higher thiol contents (Figure 2c). Gel fraction and swelling measurements were conducted to give information into the cross-linking state of these materials (Figure S3). After reaching a maximum gel fraction of 88.9 ± 0.58% at a vinyl/thiol ratio of 1:2, the gel fraction progressively decreased with increasing thiol content, reaching a value of 48.9 ± 1.73% at a vinyl/thiol ratio of 1:10. Within this composition range, the swelling ratio increased from 4.35 ± 0.04 to 25.8 ± 1.79. These

observations follow expected trends in the properties of off-stoichiometry elastomers in which the cross-link density decreases with an increasing degree of super-stoichiometry.[58]

A control experiment was carried out using a dithiol backbone and polyvinyl cross-linkers to test the effect of excess vinyl groups. As the vinyl/thiol ratio increased from 1:1 to 20:1, no photoswitching is observed (Figure S4). This observation that photodynamic behavior is promoted by excess thiols, but not excess vinyls, indicates that free thiols are necessary to enable the desired photoswitching reaction.

To probe the effect of thiol functionality, photo-CANs were prepared with a fixed vinyl/thiol ratio of 1:3 and varying ratio of polythiol/dithiol oligomers (Figure 2d). As the dithiol proportion increased, the photoinduced relative change in G' increased (Figure 2e and S5). Consistent with the role of dithiols as chain extenders rather than cross-linkers,[59] G' (UV off) decreases with increasing dithiol content (Figure 2f). Similarly, the viscosity (UV on) decreases with an increasing dithiol content. The strong dependence of photoswitching behavior on thiol functionality suggests that a polymer network structure has a strong impact on its photodynamic behavior. According to the theory by Flory,[60] the gel point shifts to a larger proportion of converted bonds as the precursor functionality decreases. Hence, a decreasing proportion of dynamic bonds are needed to induce the liquid state in systems with lower precursor functionality. By combining the results of experiments varying thiol content (Figure 2b) and thiol functionality (Figure 2e) on the same plot (Figure S6), we find overlapping trends in the photoinduced change in G' versus G' (UV off), confirming the important effect of cross-link density on the switching process.

Next, we investigated the effects of divinyl molecular weight using oligomers of varying molecular weights (Figure 2g). We focused on a 75:25 ratio of polythiol/dithiol due to its favorable photoswitching behavior demonstrated in Figure 2e. Samples prepared with 0.8 and 9.4 kDa divinyl oligomers exhibited larger photoinduced changes in G' than those with 28 kDa (Figure 2h). G' (UV off) and viscosity (UV on) both increased with the molecular weight of the divinyl component (Figure 2g). This ability to tune the viscosity of the sol state during UV exposure could be deployed for applications in which specific viscosities are required. The results in Figure 2f−i do reveal a potential limitation of our photo-CANs, which is limited to $G' < 100$ kPa. However, we note that this modulus range is compatible with several targeted applications, including dielectric elastomer actuators,[61] pneumatic soft robots,[62] cell culture substrates,[63] and wearable electronics.[64]

We studied the stability and longevity of photoswitching using different initiators in photo-CANs containing a 1:3 vinyl/thiol ratio, polythiol/dithiol ratio of 75:25, and 9.4 kDa divinyl groups (Figure 3a−d) and different light intensities (Figure 3f−h). Type I radical initiators break into two fragments—each of which have one carbon-centered radical. Type II initiators interact with a sensitizer that can donate an electron or hydrogen atom to generate a radical on the sensitizer such as a nitrogen or thiol group. Type I initiators enable large switching magnitudes (Figure 3c and S7) with 2-hydroxy-2-methyl-1-phenyl-propan-1-one (HMPP) exhibiting the best combination of large switching magnitude and stability over many cycles. By contrast, type II initiators induce curing but not switching. While the identification of the precise reaction intermediates will be the subject of future work, we expect that this difference between type I and type II initiators is related to the difference in energy of the radicals that are produced. Type I initiators
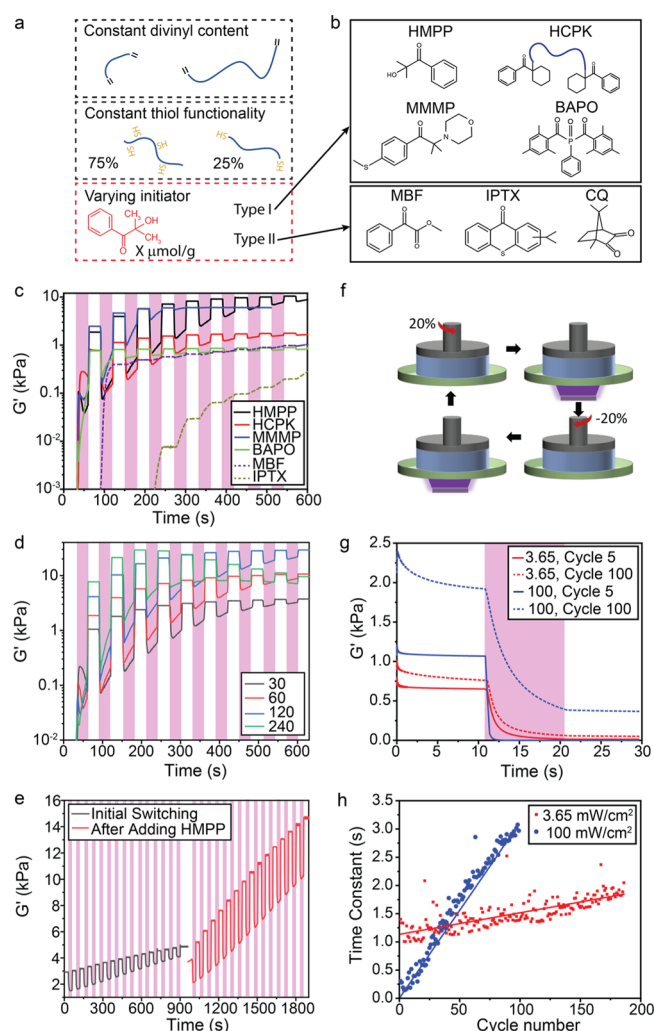

Figure 3. (a) Schematic of photo-CANs with a constant divinyl content, thiol functionality, and varying photoinitiator composition. (b) Molecular structure of different photoinitiators, where HCPK refers to PDMS-functionalized 1-hydroxycyclohexyl phenyl ketone (Irgacure 184), MMMP refers to 2-methyl-4′-(methylthio)-2-morpholinopropiophenone, BAPO refers to phenylbis(2,4,6-trimethylbenzoyl)-phosphine oxide, MBF refers to methylbenzoylformate, and IPTX refers to isopropyl thioxanthone. (c) Comparison of optical switching for type I photoinitiators (solid lines) and type II photoinitiators (dashed lines). (d) G' vs time during photoswitching for materials with different concentrations of HMPP initiator. The legend indicates the concentration of HMPP in μmol/cm^3. (e) G' vs time during photoswitching for materials with more initiator added after 15 cycles at 16.7 mW/cm^2. (f) Schematic of the cyclic testing, which consisted of a series of stress relaxation measurements at 20% strain with a UV exposure time of 10 s. (g) Stress relaxation measurements (cycles 5 and 100 are shown) during photoswitching of systems subjected to different UV light intensities of 3.65 mW/cm^2 and 100 mW/cm^2, respectively. The legend indicates the light intensity (in mW/cm^2) and cycle number. (h) Time constants as a function of cycle number obtained from the stress relaxation measurements during cycling. [Note: The solid lines are a linear fit to the data. All measurements were conducted using the optimized composition consisting of a divinyl oligomer with 9.4 kDa, a vinyl/thiol ratio of 1:3, and a polythiol/dithiol molar ratio of 75:25.]

generate carbon-centered radicals that have energies that are higher than that of a typical C−S bond. Type II initiators generate thiol-centered radicals that have energies lower than

that of a C−S bond, which may be insufficient to induce the dynamic bonding.[65]

While the type of photoinitiator determines the free radicals formed and how they react with other molecules, the amount of the photoinitiator determines the free radical concentration. Consequently, we observe an increase in switching magnitude as the HMPP concentration increases from 30 to 240 μmol/cm^3 (Figure 3d and S8). We also find that adding more HMPP can enhance the magnitude of subsequent switching cycles. For example, the magnitude of switching decreased during the first 15 cycles due to the photoinduced depletion of the initiator but then increased upon adding additional HMPP (Figure 3e and S9). This striking observation reveals that photoswitching behavior depends upon creating free radicals, which can be replenished. Our findings also indicate that lower switching magnitudes are observed when illuminated in the UVAB portion of the spectrum. Indeed, negligible switching is observed when illuminated in the 400−500 nm range because HMPP absorbs between 245 and 331 nm rather than these longer wavelengths[66] (Figure S10).

The cycle life of our photo-CANs were measured by the UV-induced stress relaxation at 20% shear strain (Figure 3f). At a low UV intensity of 3.65 mW/cm^2, their stress relaxation behavior at cycle 5 and cycle 100 were similar (Figure 3g). Over 180 cycles, the time constant for relaxation exhibits a moderate increase from 1.2 to 1.8 s (Figure 3h), indicative of reversible dynamic switching. However, at a higher UV intensity of 100 mW/cm^2, the materials exhibit fast stress relaxation in the first several cycles, but the time constant for stress relaxation increases linearly with a cycle number from less than 0.2 s at low cycle numbers to greater than 3 s at 100 cycles. The faster stress relaxation at higher intensity UV is presumably due to the larger proportion of dynamic bonds induced by the higher concentration of photoinduced radicals. However, the higher UV intensity also depletes the initiator more quickly, limiting the cycle life of the switching behavior. In addition, the increase in G' (UV off) with increasing cycles indicates progressive curing due to side reactions.[38] By the 50th cycle, the elastomer no longer reaches full stress relaxation within 10 s.

The dependence of the rheology on the oscillation frequency can give further insights into the dynamics of CANs (Figure 4a). When illuminated by UV light with an intensity of 16.3 mW/cm^2, the slope of log G'/log ω = 2 and log G''/log ω = 1 at frequencies lower than the cross-over point is indicative of a Maxwell fluid composed of either uncross-linked or lightly cross-linked polymers,[67] supporting the liquid-like nature of the dynamic state. Absent UV light, the photo-CANs exhibit the mechanical properties of typical elastomers. This nearly ideal entropic elasticity is a common trait in elastomer-based CANs[37] and manifests as minimal hysteresis in the tensile stress−strain behavior (Figure 4b), minimal stress relaxation (Figure 4c), and minimal creep (Figure S11).

The mechanical properties of thermally activated dynamic networks (e.g., disulfides,[68] hydrogen bonded networks,[18,69] and vitrimers[28]) are sensitive to the temperature. By contrast, the shear modulus of our photo-CANs (Figure 4d) remains nearly constant as the temperature is increased from 25 to 100 °C. In comparison, systems based on disulfide bonds typically soften and begin to flow at ∼70 °C,[70−73] indicting that the presence of dynamic disulfides are not the dominant factor leading to the observed reversibility of our photo-CANs. The small increase in G' with the temperature is consistent with entropic elasticity ($G' = kT/M_c$), where M_c is the molecular weight between cross-
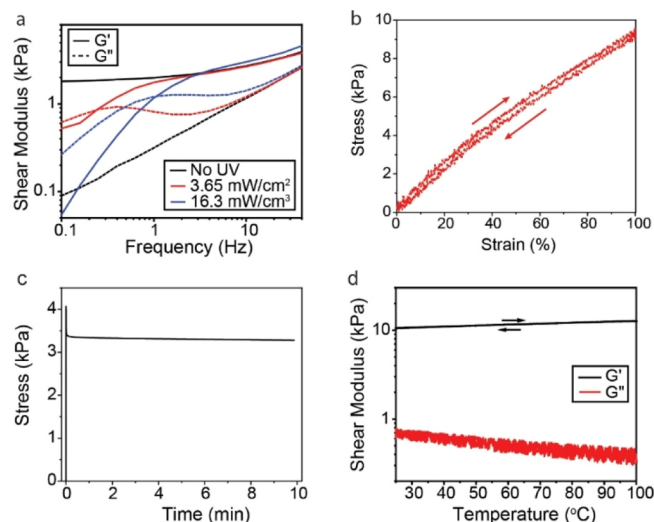

Figure 4. (a) Shear modulus as a function of frequency for the optimized composition consisting of a divinyl oligomer with 9.4 kDa, a vinyl/thiol ratio of 1:3, and a polythiol/dithiol molar ratio of 75:25 with and without UV light. (b) Stress vs strain measurements for this system. (c) Shear stress relaxation for this system in the absence of UV light. (d) Shear modulus as a function of temperature for this system.

links. The stable mechanical properties of UV-induced dynamic covalent bonding in response to thermal perturbations make them appropriate for applications, where the thermal cycling of devices is necessary, such as thermally activated actuators.[42,43] The thermal stability of the elastomer also suggests that UV-induced thermal heating of the material is likely not a contributing factor to the switching behavior.

The dramatic decrease in viscosity when photoilluminated, together with the recovery of their properties after the UV light is turned off, suggest several applications, including photo-bondable/de-bondable adhesives, damage recovery and healing, and remoldable, conformable devices, as illustrated in Figure 5. To explore damage recovery and healing under UV light, dog-bone samples of an optimized elastomer were cast and cured for tensile stress−strain characterization. Three samples were cut, the cut surface were placed together and then illuminated for 60 s. A video of the healing process is included as Video S2. As indicated in Figure 5a, the stress−strain behavior of the as-cast samples and the healed samples were very similar. The healing efficiency in terms of the elongation at break is 94%. Significantly, the broken and healed samples generally failed in locations other than the initially cut region (marked), indicating that the healed location is not the weakest section. There was a slight increase in the elastic modulus after healing, probably due to continued simultaneous curing and switching of the network, as shown in Figure 2. Strikingly, when stretched to 100% strain, the original and healed elastomers exhibited very small hysteresis values of 6 and 5% of a full scale output, respectively (Figure S12).

To determine the flow stress under UV illumination, samples were stretched at constant displacement rates of 1 mm/s (Figure 5b) and 5 mm/s (Figure S13, Video S3) while measuring the force. The flow stress behavior is highly dependent on material composition, as shown in Figure 5b. For the PDMS-based photo-CANs composed of a 1:7 vinyl/thiol ratio with only polythiols and different divinyl oligomers, photoplastic behavior was observed illustrating a constant flow stress following an initial yield drop once the UV was turned on (Figure 5b(i)). The
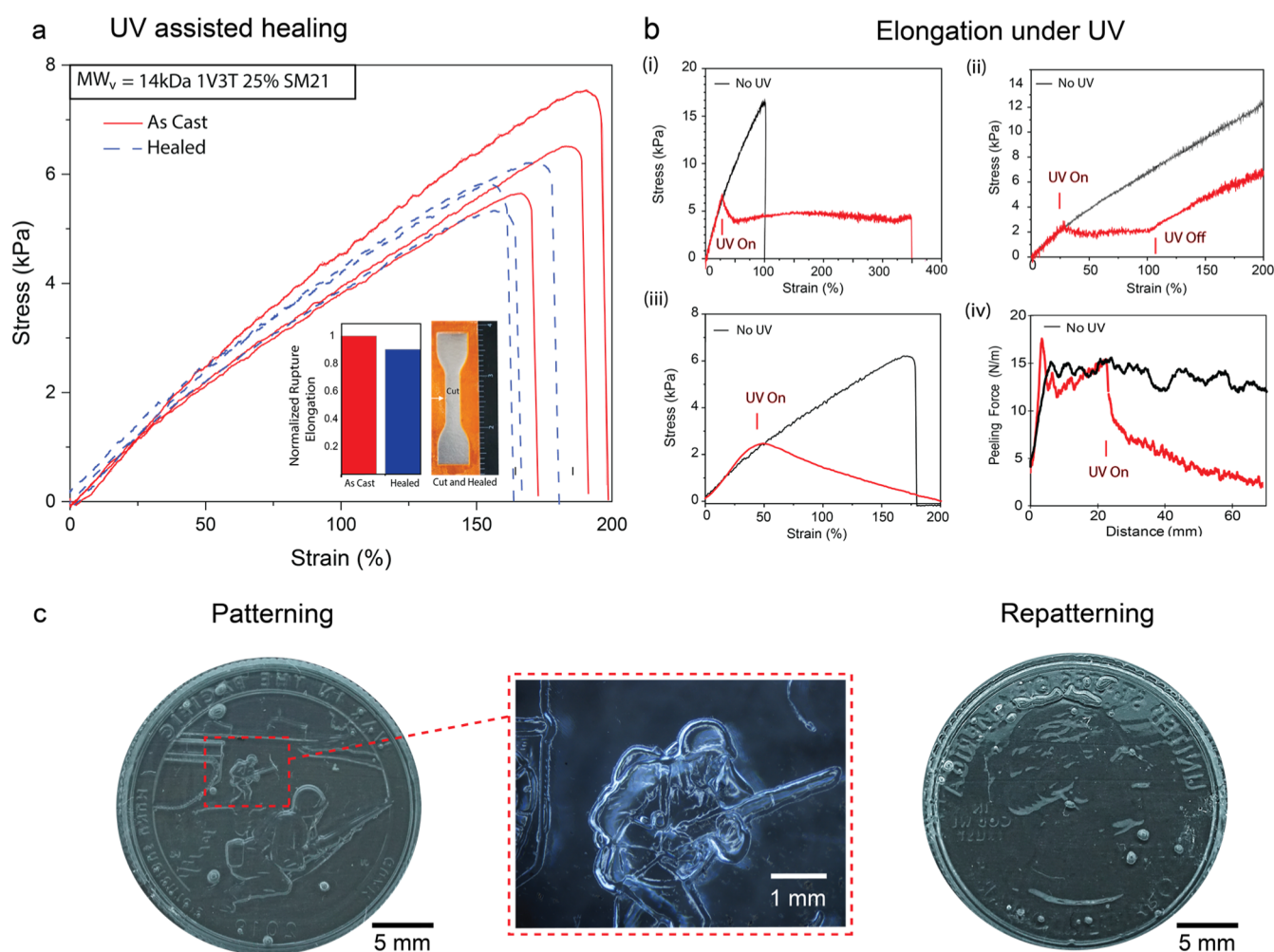
Figure 5. (a) Comparison of the tensile stress–strain behavior of as-cast and cut/healed photo-CANs composed of a vinyl/thiol ratio of 1:3, a molar ratio of polythiol/dithiol of 75:25, and a 14 kDa divinyl oligomer. The cut samples were healed by photoillumination for 60 s. (b) (i,ii) Stress measured at a 1 mm/s displacement rate for photo-CANs exposed to UV and no UV, respectively, for a 9.4 kDa divinyl oligomer with a vinyl/thiol ratio of 1:7, and cured for 60 and 30 s. (iii) Comparison of the stress–strain behavior of the 14 kDa divinyl oligomer having a vinyl/thiol ratio of 1:3 and a molar ratio of polythiol/dithiol of 75:25, once UV was turned on. Observations indicate that under UV, the sample sagged under its own weight. (iv) Peeling force as a function of the clamp distance for two PE substrates (20 μm) bonded together with a photo-CAN consisting of 9.4 kDa PDMS divinyl at a 1:3 vinyl/thiol ratio with 75:25 polythiol/dithiols. Red curve is for the bonded substrate exposed to UV light of 100% intensity after a displacement of 20 mm. (c) Photoinduced re-molding and re-patterning of silicone elastomer networks. Repeatable patterning and repatterning of photo-CANs with different surface engravings, showing the high resolution of features.

elongation under UV was considerably larger than without the UV illumination (black curve) and it finally failed by abrupt necking. The same material cured for only 30 s exhibited the same photoplastic behavior until the UV was turned off and then the initial elastic response was recovered (Figure 5b(ii)). At the same testing deformation rate, the same material but having a 1:3 vinyl/thiol ratio, stretched under its own weight once the UV was turned on so the apparent flow stress steadily decreased with continued displacement (Figure 5b(iii)).

Notably, the adhesive strength of the photo-CANs is reduced under UV illumination (Figure 5b(iv)). In the absence of UV light, the peeling force is almost constant with the peeling displacement (black curve) indicating steady-state peeling. When UV light is turned on at 30 s, the peeling force (red curve) drops to nearly zero. Viscous necking of this elastomer as it transitions to a liquid-like state can be seen in Video S4.

The reduced viscosity and liquid-like behavior under UV exposure provides opportunities for processing at ambient temperatures without heating. Typically, an uncured elastomer

can be poured onto a surface, where it flows to match the surface features that are then imprinted onto the cured elastomer. While the same pre-cure patterning can be achieved with the photodynamic elastomers in the absence of UV light, post-curing patterning can also be achieved under UV light. For instance, a flat cured sheet of the optimized elastomer with 9.4 kDa divinyl oligomer is placed on coin A and then illuminated (Figure 5c). After exposure and peeling away this elastomer, the surface conforms to that of the coin. When repeated on another area of the coin, the original imprinted features are replaced by features corresponding to the new location on the coin. Our light-processable polymers have several advantages over prior demonstrations.[15] First, thermally processable elastomers can build up stress during the process of cooling from the solidification temperature to room temperature. By using light-based processing at room temperature, this stress buildup can be avoided. Second, the energy required for light-induced remolding can be lower because stress relaxation can be induced with exposure doses as low as 36.5 mJ/cm^2. By comparison,

assuming a heat capacity of 1.38 kJ/kg K, PDMS-based, thermal CANs require approximately 4.3 J/cm^2 to heat them from 25 to 90 °C. Hence, photo-CANs may be of significant interest for the sustainable manufacturing of functional elastomers and devices.

3. CONCLUSIONS

A new class of radical-induced covalent adaptive networks based on dynamic thiol−ene chemistries has been demonstrated. Large and reversible photoswitching from a network gel state to a sol state are observed over a range of thiol-to-alkene moieties and molecular weights at ambient temperature. Their fast photoswitching behavior is attributed to a dynamic covalent bonding associated with the creation of radical species under UV illumination. The transition leads to several photoplastic effects including UV-induced healing of damage, large plastic deformation, and decreased viscosity. These have potential applications as debondable adhesives, remoldable elastomers, and in damage recovery for extended life applications.

4. EXPERIMENTAL METHODS

4.1. Photo-CANs. PEG-PES elastomers were prepared as described previously.[55] In brief, a divinyl component [tri(ethylene glycol)divinyl ether, Aldrich] and a dithiol component [2,2′-(ethylenedioxy)-diethanethiol, Aldrich] were combined in a stoichiometric ratio of 10:9 with 1 wt % of UV initiator Irgacure 651 (2,2-dimethoxy-2-phenylacetophenone). After UV polymerization for 10 min, the resulting vinyl-terminated oligomers have a molecular weight of ∼3.7 kDa. These PEG-PES oligomers were combined with tetrathiols [pentaerythritol tetrakis(3-mercaptopropionate), Aldrich] at a vinyl/thiol ratio of 1:2. This ratio resulted in 5 g of 3.7 kDa PEG-PES oligomers being combined with 0.67 g of tetrathiols. PUA (CN9028) was received from Sartomer. We added 0.45 g of tetrathiols per 5 g of CN9028, which is sufficient to give rise to the photodynamic behavior depicted in Figure 1c.

Vinyl-terminated PDMS (DMS-V*XX*, where *XX* is 05 for 0.8 kDa oligomers, 22 for 9.4 kDa oligomers, PDV for 14 kDa oligomers, and 31 for 28 kDa oligomers), polyfunctional mercaptopropyl-functionalized PDMS (SMS-042), and bifunctional PDMS end-terminated with thiols (DMS-SM21) were purchased from Gelest. Irgacure 1173 (2-hydroxy-2-methyl propiophenone, HMPP) was purchased from Sigma-Aldrich. In the optimized PDMS composition (Figure 1b), 0.94 g of SMS-042 and 1.06 g of DMS-SM21 were mixed together using a Thinky Mixer ARE-310 for 1 min. Vinyl terminated PDMS was added at a 1:3 vinyl/thiol stoichiometric concentrations(1.33 g) with 1 wt % photoinitiator and mixed homogeneously at 2000 rpm for 5 min. After mixing, the vials are covered with aluminum foil to prevent any photoinitiator activation. For compositions with high vinyl contents, 10 kDa PDMS end terminated with thiols (DMS-SM21 from Gelest) was combined with a vinyl-functional cross-linker (VDT-431 from Gelest) in vinyl/thiol ratios from 1:1 to 20:1.

Several photoinitiators were used, including MMMP, BAPO, MBF, IPTX, and camphorquinone (CQ) purchased from Sigma-Aldrich. 1-Hydroxycyclohexyl phenyl ketone (HCPK, Irgacure 184) was not sufficiently soluble in PDMS, so it was chemically modified with PDMS. HCPK and epoxy-functionalized PDMS (DMS-E12 from Gelest) were combined in a 1:1 ratio of HCPK to epoxy groups in a vial. Chloroform was added as a cosolvent, and the mixture was stirred at 50 °C for 2 days. After evaporation of the chloroform, the PDMS-modified HCPK did not show any phase separation.

Samples were prepared with the optimized PDMS composition (4 g of 9.4 kDa divinyl PDMS, 2.82 g of polythiol PDMS, and 3.19 g of dithiol PDMS) and 60 μmol/g of the initiator. 8 g of dichloromethane was then added to the composition and mixed in a speedmixer for 10 min to dissolve the initiator. The samples were mixed for 10 min to evaporate dichloromethane.

4.2. Gel Fraction and Swelling Measurements. The elastomers were cured at 100% intensity for 60 s inside the photorheometer with a thickness of 1 mm. Dimensions and mass of the cured elastomers were recorded. The elastomers were immersed in toluene for 3 days and stirred every 12 h. Toluene was decanted, and dimension and mass of the samples were measured while elastomers were swelled. Then, elastomers were dried at 50 °C under vacuum for 5 h. The mass and dimensions of the dried elastomer were recorded once values stabilized.

4.3. Photorheology Measurements. The photosource used was an Omnicure model S2000, which emits a broadband spectra from 250 to 600 nm. The Omnicure was connected to a photorheology attachment on a TA Discovery DHR-3 rheometer equipped with a 20 mm flat steel plate. In the photorheometer system, the Omnicure output an irradiance of 100 mW/cm^2 in the UV range (<400 nm). The irradiance was altered by changing the intensity of the Omnicure. Rheology measurements were conducted with a gap of 500 μm. Cross-linking studies were done while measuring the rheology at an oscillation strain of 1% and frequency of 1 Hz. Stress relaxation measurements were conducted by applying 20% strain and turning on the UV light. Creep measurements were conducted by applying a stress equal to the shear modulus of the cross-linked material. Temperature-dependent measurements were completed by cross-linking the sample for 60 s at 100 mW/cm^2, raising the top plate (with the sample still adhered), and replacing the photorheology attachment with a Peltier plate. After lowering the top plate so that the sample was in contact with a Peltier plate, measurements were conducted at an oscillation strain of 1% and a frequency of 1 Hz, while the temperature was ramped at a speed of 2 °C/min.

4.4. Mechanical Property Measurements. To quantify damage recovery and healing under UV, dog-bone samples of an optimized elastomer (3 mm thick) were cast and cured for tensile stress−strain characterization. The selected composition was a 14 kDa divinyl PDMS at a 1:3 vinyl/thiol ratio with 75:25 polythiol/dithiol ratio and 1 wt % (∼60 μmol/cm^3) of the HMPP photoinitiator. All samples were first cured under nitrogen for 150 s at 35 mW/cm^2 UV exposure. Some samples were tested in their cast and cured state to provide reference mechanical data. Others were cut in half with a knife and then placed in contact for healing. Under nitrogen, the cut samples were exposed to broadband UV light for 60 s at 35 mW/cm^2 exposure. After the samples were healed, a marker indicated the place of healing. Tensile stress−strain curves were performed with the test samples in a horizontal direction. In all cases, the tensile tests were performed at a nominal displacement rate of 1 mm/s, and the load recorded with a 10 N load cell. In a video recording, the material was observed to flow while the UV was on and heal the cut and then solidify when the UV is turned off (Video S2). The mechanical properties of these samples were then measured and compared to the as-cast samples.

Elastomer samples of 9.4 kDa PDMS divinyl at a 1:3 vinyl/thiol ratio with 75:25 polythiol/dithiols with 1 wt % HMPP were made to quantify the peeling force with and without exposure to UV. Elastomer samples (60 mm × 10 mm × 150 μm) were cured under nitrogen, for 150 s at 35 mW/cm^2 on 20 μm of the polyethylene film substrate. After curing, another layer of 20 μm of the PE film was placed on top and UV was exposed through the top substrate for an additional 30 s. Peeling force as a function of the clamp distance was measured using an in-house tensile setup with 50 N load cell at a displacement rate of 1 mm/s. After 20 mm displacement, the UV was turned on and debonding measured with the UV source 10 cm directly above the sample at 100% intensity.

4.5. Molding/Remolding of Photo-CANs. Elastomer samples of 9.4 kDa PDMS divinyl at a 1:3 vinyl/thiol ratio with 75:25 polythiol/dithiols at 1 wt % HMPP were made to demonstrate patterning and repatterning under UV exposure. Elastomers (1 mm thick) were cured under nitrogen for 150 s at 35 mW/cm^2 on the ITO/PET substrate. The sample was placed above a quarter-dollar coin, and UV was exposed through the ITO/PET for 60 s. When the elastomer is removed from the coin, microscopy shows similar features to the surface of the coin. The same elastomer sample was then placed onto another coin with different surface features. Under the same UV exposure, the elastomer is able to repattern from the features of one coin to another.

■ ASSOCIATED CONTENT

Ⓢ︎ Supporting Information

The Supporting Information is available free of charge at https://pubs.acs.org/doi/10.1021/acsami.1c22287.

G_{UVoff}' and UV-induced change in G' for different vinyl/thiol ratios, hypothesized contributions to the profile of G' over time during UV exposure, gel fractions and swelling ratios for compositions with different vinyl/thiol ratios, photorheology data on compositions with high vinyl contents, G_{UVoff}' and UV-induced change in G' for different ratios of polythiols/dithiols, relationship between G' and the UV-induced change in G', G_{UVoff}' and UV-induced change in G' for different initiators, G_{UVoff}' and UV-induced change in G' for different contents of HMPP photoinitiator, UV-induced change in G' for 15 cycles before and after the addition of additional HMPP initiators, G' during periodic exposure to different wavelengths of light, creep measurements on a PDMS photo-CAP, tensile stress−strain measurements on a photo-CAP without UV exposure showing hysteresis, and a tensile measurement on a photo-CAP during UV exposure (PDF)

Flow behavior of photo-CAN (MP4)

UV-induced healing (MP4)

Tensile test with UV exposure (MP4)

Peel tests with UV exposure (MP4)

■ AUTHOR INFORMATION

Corresponding Authors

　Alex Chortos − *School of Engineering and Applied Sciences, Harvard University, Cambridge, Massachusetts 02138, United States; School of Mechanical Engineering, Purdue University, West Lafayette, Indiana 47907, United States;* ⓘ orcid.org/0000-0003-3976-5257; Email: achortos@purdue.edu

　David R. Clarke − *School of Engineering and Applied Sciences, Harvard University, Cambridge, Massachusetts 02138, United States;* Email: clarke@seas.harvard.edu

Authors

　Kezi Cheng − *School of Engineering and Applied Sciences, Harvard University, Cambridge, Massachusetts 02138, United States*

　Jennifer A. Lewis − *School of Engineering and Applied Sciences, Harvard University, Cambridge, Massachusetts 02138, United States;* ⓘ orcid.org/0000-0002-0280-2774

Complete contact information is available at:
https://pubs.acs.org/10.1021/acsami.1c22287

Notes

The authors declare no competing financial interest.

■ ACKNOWLEDGMENTS

■ REFERENCES

(1) Shian, S.; Bertoldi, K.; Clarke, D. R. Dielectric Elastomer Based "Grippers" for Soft Robotics. *Adv. Mater.* **2015**, *27*, 6814−6819.

(2) Duduta, M.; Hajiesmaili, E.; Zhao, H.; Wood, R. J.; Clarke, D. R. Realizing the Potential of Dielectric Elastomer Artificial Muscles. *Proc. Natl. Acad. Sci. U.S.A.* **2019**, *116*, 2476−2481.

(3) Polygerinos, P.; Correll, N.; Morin, S. A.; Mosadegh, B.; Onal, C. D.; Petersen, K.; Cianchetti, M.; Tolley, M. T.; Shepherd, R. F. Soft Robotics: Review of Fluid-driven Intrinsically Soft Devices; Manufacturing, Sensing, Control, and Applications in Human-Robot Interaction. *Adv. Eng. Mater.* **2017**, *19*, 1700016.

(4) Majidi, C. Soft-Matter Engineering for Soft Robotics. *Adv. Mater. Technol.* **2019**, *4*, 1800477.

(5) Chortos, A.; Liu, J.; Bao, Z. Pursuing Prosthetic Electronic Skin. *Nat. Mater.* **2016**, *15*, 937−950.

(6) Wang, X.; Dong, L.; Zhang, H.; Yu, R.; Pan, C.; Wang, Z. L. Recent Progress in Electronic Skin. *Adv. Sci.* **2015**, *2*, 1500169.

(7) Yang, J.; Steck, J.; Bai, R.; Suo, Z. Topological Adhesion II. Stretchable Adhesion. *Extreme Mech. Lett.* **2020**, *40*, 100891.

(8) Wang, Z.; Xiang, C.; Yao, X.; Le Floch, P.; Mendez, J.; Suo, Z. Stretchable Materials of High Toughness and Low Hysteresis. *Proc. Natl. Acad. Sci. U.S.A.* **2019**, *116*, 5967−5972.

(9) Liu, Q.; Nian, G.; Yang, C.; Qu, S.; Suo, Z. Bonding Dissimilar Polymer Networks in Various Manufacturing Processes. *Nat. Commun.* **2018**, *9*, 846.

(10) Flory, P. J. Network Structure and the Elastic Properties of Vulcanized Rubber. *Chem. Rev.* **1944**, *35*, 51−75.

(11) Sun, S.; Fei, G.; Wang, X.; Xie, M.; Guo, Q.; Fu, D.; Wang, Z.; Wang, H.; Luo, G.; Xia, H. Covalent Adaptable Networks of Polydimethylsiloxane Elastomer for Selective Laser Sintering 3D Printing. *Chem. Eng. J.* **2021**, *412*, 128675.

(12) Li, Q.; Ma, S.; Lu, N.; Qiu, J.; Ye, J.; Liu, Y.; Wang, S.; Han, Y.; Wang, B.; Xu, X.; Feng, H.; Zhu, J. Concurrent Thiol−ene Competitive Reactions Provide Reprocessable, Degradable and Creep-resistant Dynamic−permanent Hybrid Covalent Networks. *Green Chem.* **2020**, *22*, 7769−7777.

(13) Suh, D.; Faseela, K. P.; Kim, W.; Park, C.; Lim, J. G.; Seo, S.; Kim, M. K.; Moon, H.; Baik, S. Electron tunneling of hierarchically structured silver nanosatellite particles for highly conductive healable nanocomposites. *Nat. Commun.* **2020**, *11*, 2252.

(14) Li, X.; Yu, R.; He, Y.; Zhang, Y.; Yang, X.; Zhao, X.; Huang, W. Self-healing Polyurethane Elastomers Based on a Disulfide Bond by Digital Light Processing 3D Printing. *ACS Macro Lett.* **2019**, *8*, 1511−1516.

(15) Zheng, P.; McCarthy, T. J. A Surprise from 1954: Siloxane Equilibration is a Simple, Robust, and Obvious Polymer Self-healing Mechanism. *J. Am. Chem. Soc.* **2012**, *134*, 2024−2027.

(16) Osthoff, R. C.; Bueche, A. M.; Grubb, W. T. Chemical Stress-Relaxation of Polydimethylsiloxane Elastomers. *J. Am. Chem. Soc.* **1954**, *76*, 4659−4663.

(17) Solouki Bonab, V.; Karimkhani, V.; Manas-Zloczower, I. Ultra-Fast Microwave Assisted Self-Healing of Covalent Adaptive Polyurethane Networks with Carbon Nanotubes. *Macromol. Mater. Eng.* **2019**, *304*, 1800405.

(18) Chen, Y.; Tang, Z.; Zhang, X.; Liu, Y.; Wu, S.; Guo, B. Covalently Cross-linked Elastomers with Self-healing and Malleable Abilities Enabled by Boronic Ester Bonds. *ACS Appl. Mater. Interfaces* **2018**, *10*, 24224−24231.

(19) Fortman, D. J.; Brutman, J. P.; De Hoe, G. X.; Snyder, R. L.; Dichtel, W. R.; Hillmyer, M. A. Approaches to Sustainable and Continually Recyclable Cross-linked Polymers. *ACS Sustainable Chem. Eng.* **2018**, *6*, 11145−11159.

(20) Hartmann, F.; Baumgartner, M.; Kaltenbrunner, M. Becoming Sustainable, the New Frontier in Soft Robotics. *Adv. Mater.* **2021**, *33*, 2004413.

(21) Zheng, N.; Xu, Y.; Zhao, Q.; Xie, T. Dynamic Covalent Polymer Networks: A Molecular Platform for Designing Functions beyond Chemical Recycling and Self-Healing. *Chem. Rev.* **2021**, *121*, 1716−1745.

(22) Zhang, Y.; Broekhuis, A. A.; Picchioni, F. Thermally Self-healing Polymeric Materials: The Next Step to Recycling Thermoset Polymers? *Macromolecules* **2009**, *42*, 1906−1912.

(23) Kloxin, C. J.; Scott, T. F.; Adzima, B. J.; Bowman, C. N. Covalent Adaptable Networks (CANs): a Unique Paradigm in Cross-linked Polymers. *Macromolecules* **2010**, *43*, 2643−2653.

(24) Kennedy, J. P.; Castner, K. F. Thermally Reversible Polymer Systems by Cyclopentadienylation. I. A Model for Termination by Cyclopentadienylation of Olefin Polymerization. *J. Polym. Sci., Polym. Chem. Ed.* **1979**, *17*, 2039−2054.

(25) Adzima, B. J.; Aguirre, H. A.; Kloxin, C. J.; Scott, T. F.; Bowman, C. N. Rheological and Chemical Analysis of Reverse Gelation in a Covalently Cross-linked Diels−Alder Polymer Network. *Macromolecules* **2008**, *41*, 9112−9117.

(26) Polgar, L. M.; Van Duin, M.; Broekhuis, A. A.; Picchioni, F. Use of Diels−Alder Chemistry for Thermoreversible cross-linking of Rubbers: the Next Step Toward Recycling of Rubber Products? *Macromolecules* **2015**, *48*, 7096−7105.

(27) Otsuka, H. Reorganization of Polymer Structures Based on Dynamic Covalent Chemistry: Polymer Reactions by Dynamic Covalent Exchanges of Alkoxyamine Units. *Polym. J.* **2013**, *45*, 879−891.

(28) Denissen, W.; Rivero, G.; Nicolaÿ, R.; Leibler, L.; Winne, J. M.; Du Prez, F. E. Vinylogous Urethane Vitrimers. *Adv. Funct. Mater.* **2015**, *25*, 2451−2457.

(29) Chen, X.; Dam, M. A.; Ono, K.; Mal, A.; Shen, H.; Nutt, S. R.; Sheran, K.; Wudl, F. A Thermally Re-mendable Cross-linked Polymeric Material. *Science* **2002**, *295*, 1698−1702.

(30) Saed, M. O.; Terentjev, E. M. Siloxane Crosslinks with Dynamic Bond Exchange Enable Shape Programming in Liquid-Crystalline Elastomers. *Sci. Rep.* **2020**, *10*, 6609.

(31) Lu, Y.-X.; Tournilhac, F.; Leibler, L.; Guan, Z. Making Insoluble Polymer Networks Malleable via Olefin Metathesis. *J. Am. Chem. Soc.* **2012**, *134*, 8424−8427.

(32) Pei, Z.; Yang, Y.; Chen, Q.; Terentjev, E. M.; Wei, Y.; Ji, Y. Mouldable Liquid-Crystalline Elastomer Actuators with Exchangeable Covalent Bonds. *Nat. Mater.* **2014**, *13*, 36−41.

(33) Scott, T. F.; Schneider, A. D.; Cook, W. D.; Bowman, C. N. Photoinduced Plasticity in Cross-linked Polymers. *Science* **2005**, *308*, 1615−1617.

(34) Scott, T. F.; Draughon, R. B.; Bowman, C. N. Actuation in Crosslinked Polymers via Photoinduced Stress Relaxation. *Adv. Mater.* **2006**, *18*, 2128−2132.

(35) Van Damme, J.; van den Berg, O.; Brancart, J.; Vlaminck, L.; Huyck, C.; Van Assche, G.; Van Mele, B.; Du Prez, F. Anthracene-based Thiol−ene Networks with Thermo-degradable and Photo-reversible Properties. *Macromolecules* **2017**, *50*, 1930−1938.

(36) Lendlein, A.; Jiang, H.; Jünger, O.; Langer, R. Light-induced Shape-memory Polymers. *Nature* **2005**, *434*, 879−882.

(37) McBride, M. K.; Worrell, B. T.; Brown, T.; Cox, L. M.; Sowan, N.; Wang, C.; Podgorski, M.; Martinez, A. M.; Bowman, C. N. Enabling Applications of Covalent Adaptable Networks. *Annu. Rev. Chem. Biomol. Eng.* **2019**, *10*, 175−198.

(38) Frisch, H.; Marschner, D. E.; Goldmann, A. S.; Barner-Kowollik, C. Wavelength-Gated Dynamic Covalent Chemistry. *Angew. Chem., Int. Ed.* **2018**, *57*, 2036−2045.

(39) Amamoto, Y.; Kamada, J.; Otsuka, H.; Takahara, A.; Matyjaszewski, K. Repeatable Photoinduced Self-Healing of Covalently Cross-Linked Polymers through Reshuffling of Trithiocarbonate Units. *Angew. Chem., Int. Ed.* **2011**, *50*, 1660−1663.

(40) Cook, W. D.; Chen, F.; Nghiem, Q. D.; Scott, T. F.; Bowman, C. N.; Chausson, S.; Le Pluart, L. Photo-Plasticity in Thiol-ene Network Polymers—A Review. *Macromol. Symp.* **2010**, *291−292*, 50−65.

(41) Sowan, N.; Cox, L. M.; Shah, P. K.; Song, H. B.; Stansbury, J. W.; Bowman, C. N. Dynamic Covalent Chemistry at Interfaces: Development of Tougher, Healable Composites through Stress Relaxation at the Resin-Silica Nanoparticles Interface. *Adv. Mater. Interfaces* **2018**, *5*, 1800511.

(42) Davidson, E. C.; Kotikian, A.; Li, S.; Aizenberg, J.; Lewis, J. A. 3D Printable and Reconfigurable Liquid Crystal Elastomers with Light-Induced Shape Memory via Dynamic Bond Exchange. *Adv. Mater.* **2020**, *32*, 1905682.

(43) McBride, M. K.; Martinez, A. M.; Cox, L.; Alim, M.; Childress, K.; Beiswinger, M.; Podgorski, M.; Worrell, B. T.; Killgore, J.; Bowman, C. N. A Readily Programmable, Fully Reversible Shape-switching Material. *Sci. Adv.* **2018**, *4*, No. eaat4634.

(44) Hoyle, C. E.; Bowman, C. N. Thiol-Ene Click Chemistry. *Angew. Chem., Int. Ed.* **2010**, *49*, 1540−1573.

(45) Kade, M. J.; Burke, D. J.; Hawker, C. J. The Power of Thiol-ene Chemistry. *J. Polym. Sci., Part A: Polym. Chem.* **2010**, *48*, 743−750.

(46) Kharasch, M. S.; Nudenberg, W.; Mantell, G. J. Reactions of Atoms and Free Radicals in Solution. XXV. The Reactions of Olefins with Mercaptans in the Presence of Oxygen. *J. Org. Chem.* **1951**, *16*, 524−532.

(47) Podgórski, M.; Huang, S.; Bowman, C. N. Additive Manufacture of Dynamic Thiol−ene Networks Incorporating Anhydride-Derived Reversible Thioester Links. *ACS Appl. Mater. Interfaces* **2021**, *13*, 12789−12796.

(48) Zhang, B.; Digby, Z. A.; Flum, J. A.; Chakma, P.; Saul, J. M.; Sparks, J. L.; Konkolewicz, D. Dynamic Thiol−Michael Chemistry for Thermoresponsive Rehealable and Malleable Networks. *Macromolecules* **2016**, *49*, 6871−6878.

(49) Zhang, B.; Chakma, P.; Shulman, M. P.; Ke, J.; Digby, Z. A.; Konkolewicz, D. Probing the Mechanism of Thermally Driven Thiol-Michael Dynamic Covalent Chemistry. *Org. Biomol. Chem.* **2018**, *16*, 2725−2734.

(50) Franz, J. A.; Roberts, D. H.; Ferris, K. F. Absolute Rate Expressions for Intramolecular Displacement Reactions of Primary Alkyl Radicals at Sulfur. *J. Org. Chem.* **1987**, *52*, 2256−2262.

(51) Ferris, K. F.; Franz, J. A.; Sosa, C.; Bartlett, R. J. Alkyl Radical Displacement Reactions at Sulfur: on the Question of Intermediacy in Alkylsulfuranyl Radicals. *J. Org. Chem.* **1992**, *57*, 777−778.

(52) Kampmeier, J. A.; Geer, R. P.; Meskin, A. J.; D'Silva, R. M. Free-Radical Elimination Reactions. The Reaction of Phenyl Radicals with t-Butyl Sulfide and Phenyl t-Butyl Sulfide1. *J. Am. Chem. Soc.* **1966**, *88*, 1257−1265.

(53) Dénès, F.; Schiesser, C. H.; Renaud, P. Thiols, Thioethers, and Related Compounds as Sources of C-centred Radicals. *Chem. Soc. Rev.* **2013**, *42*, 7900−7942.

(54) Baciocchi, E.; Del Giacco, T.; Gerini, M. F.; Lanzalunga, O. Rates of C−S Bond Cleavage in Tert-alkyl Phenyl Sulfide Radical Cations. *Org. Lett.* **2006**, *8*, 641−644.

(55) Chortos, A.; Hajiesmaili, E.; Morales, J.; Clarke, D. R.; Lewis, J. A. 3D Printing of Interdigitated Dielectric Elastomer Actuators. *Adv. Funct. Mater.* **2020**, *30*, 1907375.

(56) Keller, R. C. Peroxide Curing of Ethylene-Propylene Elastomers. *Rubber Chem. Technol.* **1988**, *61*, 238−254.

(57) Dluzneski, P. R. Peroxide Vulcanization of Elastomers. *Rubber Chem. Technol.* **2001**, *74*, 451−492.

(58) Mazurek, P.; Vudayagiri, S.; Skov, A. L. How to Tailor Flexible Silicone Elastomers with Mechanical Integrity: a Tutorial Review. *Chem. Soc. Rev.* **2019**, *48*, 1448−1464.

(59) Sirrine, J. M.; Meenakshisundaram, V.; Moon, N. G.; Scott, P. J.; Mondschein, R. J.; Weiseman, T. F.; Williams, C. B.; Long, T. E. Functional Siloxanes with Photo-activated, Simultaneous Chain Extension and Crosslinking for Lithography-based 3D Printing. *Polymer* **2018**, *152*, 25−34.

(60) Flory, P. J. Constitution of Three-Dimensional Polymers and the Theory of Gelation. *J. Phys. Chem.* **1942**, *46*, 132−140.

(61) Zhao, H.; Hussain, A. M.; Duduta, M.; Vogt, D. M.; Wood, R. J.; Clarke, D. R. Compact Dielectric Elastomer Linear Actuators. *Adv. Funct. Mater.* **2018**, *28*, 1804328.

(62) Wallin, T. J.; Pikul, J. H.; Bodkhe, S.; Peele, B. N.; Mac Murray, B. C.; Therriault, D.; McEnerney, B. W.; Dillon, R. P.; Giannelis, E. P.; Shepherd, R. F. Click Chemistry Stereolithography for Soft Robots that Self-heal. *J. Mater. Chem. B* **2017**, *5*, 6249−6255.

I

(63) Yeh, Y.-C.; Corbin, E. A.; Caliari, S. R.; Ouyang, L.; Vega, S. L.; Truitt, R.; Han, L.; Margulies, K. B.; Burdick, J. A. Mechanically Dynamic PDMS Substrates to Investigate Changing Cell Environments. *Biomaterials* **2017**, *145*, 23−32.

(64) Jang, K.-I.; Han, S. Y.; Xu, S.; Mathewson, K. E.; Zhang, Y.; Jeong, J.-W.; Kim, G.-T.; Webb, R. C.; Lee, J. W.; Dawidczyk, T. J. Rugged and Breathable Forms of Stretchable Electronics with Adherent Composite Substrates for Transcutaneous Monitoring. *Nat. Commun.* **2014**, *5*, 4779.

(65) Coote, M. L.; Lin, C. Y.; Zavitsas, A. A. Inherent and Transferable Stabilization Energies of Carbon-and Heteroatom-centred Radicals on the Same Relative Scale and Their Applications. *Phys. Chem. Chem. Phys.* **2014**, *16*, 8686−8696.

(66) Allen, N. S. Photoinitiators for UV and Visible Curing of Coatings: Mechanisms and Properties. *J. Photochem. Photobiol., A* **1996**, *100*, 101−107.

(67) Mezger, T. G. Behavior of Uncrosslinked Polymers. *The Rheology Handbook: For Users of Rotational and Oscillatory Rheometers*; Vincentz Network GmbH & Co. KG: Hannover, Germany, 2006; pp 187−195.

(68) Klepel, F.; Ravoo, B. J. Dynamic Covalent Chemistry in Aqueous Solution by Photoinduced Radical Disulfide Metathesis. *Org. Biomol. Chem.* **2017**, *15*, 3840−3842.
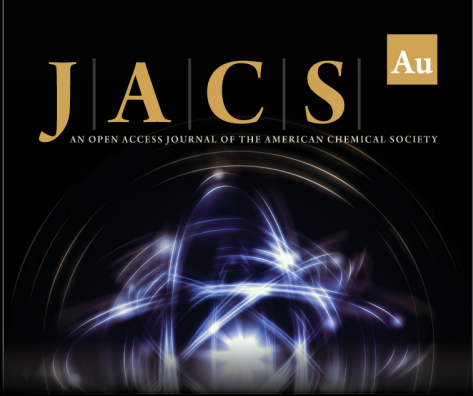
(69) Jian, X.; Hu, Y.; Zhou, W.; Xiao, L. Self-healing Polyurethane Based on Disulfide Bond and Hydrogen Bond. *Polym. Adv. Technol.* **2018**, *29*, 463−469.

(70) Endo, K.; Yamanaka, T. Copolymerization of Lipoic Acid with 1,2-dithiane and Characterization of the Copolymer as an Interlocked Cyclic Polymer. *Macromolecules* **2006**, *39*, 4038−4043.

(71) Choi, C.; Self, J. L.; Okayama, Y.; Levi, A. E.; Gerst, M.; Speros, J. C.; Hawker, C. J.; Read de Alaniz, J.; Bates, C. M. Light-Mediated Synthesis and Reprocessing of Dynamic Bottlebrush Elastomers under Ambient Conditions. *J. Am. Chem. Soc.* **2021**, *143*, 9866−9871.

(72) Fortman, D. J.; Snyder, R. L.; Sheppard, D. T.; Dichtel, W. R. Rapidly Reprocessable Cross-linked Polyhydroxyurethanes Based on Disulfide Exchange. *ACS Macro Lett.* **2018**, *7*, 1226−1231.

(73) Wu, X.; Li, J.; Li, G.; Ling, L.; Zhang, G.; Sun, R.; Wong, C.-P. Heat-triggered Poly(siloxane-urethane)s Based on Disulfide Bonds for Self-healing Application. *J. Appl. Polym. Sci.* **2018**, *135*, 46532.